RESEARCH PAPER

Enhancing Osseointegration of Cp Titanium Implants via Electrospun PCL/CH/CN Composite Coating

Khadija Sahib Hasen [1]*, ***Ghassan Abdul-Hamid Naji*** [2], ***Akram R. Jabur*** [3]

[1] *Department of Prosthodontics, College of Dentistry, University of Baghdad, Iraq*
[2] *College of Dentistry, The Iraqia University, Baghdad, Iraq*
[3] *Materials Engineering Department, University of Technology-Iraq, Baghdad, Iraq*

ARTICLE INFO

Article History:
Received 02 December 2025
Accepted 24 March 2026
Published 01 April 2026

Keywords:
Cinnamon particle
Electrospinning
Osseointegration
Titanium surface modification

ABSTRACT

In this study, we aimed to improve the osseointegration of Cp Titanium (CpTi) implants by modifying their surface properties through electrospinning a composite coating of Polycaprolactone (PCL), Chitosan (CH), and cinnamon watery extracted (CN). Various techniques, including Microscopy, chemical analysis, hydrophilicity, and biological assays, were employed to evaluate the effectiveness of this coating. The results demonstrated significant enhancements in microroughness, surface area ratio, wettability, and antibacterial activity after applying the PCL/CH/CN coating. These improvements hold promise for enhancing osseointegration by increasing torque removal rate. potentially benefiting the field of implantation, wound healing, and tissue engineering. Titanium implants are widely used in medical applications due to their biocompatibility, cost-effectiveness, and biomechanical strength. However, they are bioinert materials with limited osseointegration capabilities. This study explores the use of an electrospun composite coating to improve the surface characteristics of CpTi implants, aiming to enhance their osseointegration potential. The study involved electrospinning a PCL/CH/CN composite onto CpTi substrates. Various analytical techniques were employed, including Field-Emission Scanning Electron Microscopy (FESEM) for surface morphology examination, Energy Dispersive X-ray Spectroscopy (EDX) for chemical composition analysis, and Fourier-Transform Infrared Spectroscopy (FTIR) for functional group identification. Surface microroughness was assessed using Atomic Force Microscopy (AFM), wettability was determined via contact angle measurements, and antibacterial activity was tested against anaerobic bacteria from implant patients. Osseointegration was evaluated through torque removal measurements in a rabbit femur in vivo test. The PCL/CH/CN electrospinning coating significantly improved microroughness, surface area ratio, wettability, and exhibited antibacterial activity. These enhancements contribute to improved osseointegration, as evidenced by torque removal measurements The electrospun PCL/CH/CN composite coating offers a straightforward and rapid method to introduce topographical features while providing antibacterial properties. This promising technique has the potential to advance osseointegration in titanium implants, making it relevant for applications in wound healing and tissue engineering within the implantation field.

How to cite this article
Sahib Hasen K., Abdul-Hamid Naji G., Jabur A . Enhancing Osseointegration of Cp Titanium Implants via Electrospun PCL/CH/CN Composite Coating. J Nanostruct, 2026; 16(2):2301-2316. DOI: 10.22052/JNS.2026.02.074

* *Corresponding Author Email: Khadija.Khreibet1908@codental.uobaghdad.edu.iq*

INTRODUCTION

In recent years, herbal therapy has gained recognition for its effectiveness and safety in various medical applications. However, a significant challenge in harnessing the full potential of herbal medicine lies in its low water solubility, which limits its bioavailability. Overcoming this limitation is crucial for optimizing herbal therapy delivery [1-4].

Simultaneously, surface modification of dental implants at the nanoscale or micro scale has emerged as a promising approach to enhance bioactivity both in vitro and in vivo [5]. To achieve this, researchers have turned to the innovative technique of electrospinning. Electrospinning involves the creation of nanofibrous structures through the controlled application of an electric field to a polymer solution or melt. In this context, it offers a unique solution to the challenge of incorporating herbal medicine into implant coatings. Natural polymers, known for their biocompatibility and ability to mimic the extracellular matrix (ECM), have been favored for electrospinning applications, as they promote cell adhesion and proliferation [6]. However, these natural polymers often suffer from drawbacks such as poor mechanical properties and rapid degradation, limiting their utility. Synthetic biological polymers, on the other hand, offer a compelling solution with their uniform quality, adaptability, and stability in vivo, often being coated to enhance performance [7].

Among the diverse herbal options, cinnamon, an uncommon tropical plant from the Lauraceae family, has garnered attention in Eastern natural medicine and culinary traditions. Its extracts contain a rich array of bioactive compounds, including cinnamon aldehyde, cinnamic alcohol, cinnamic acid, cinnamate [8], along with polyphenols, protocatechuic, and coumarin [9]. Additionally, cinnamon boasts essential nutrients such as calcium, fiber, iron, and manganese [10]. Its reputation is built on its antimicrobial [11,12], antioxidant, and anti-inflammatory properties, positioning it as a valuable asset in treating conditions like cardiovascular disease and diabetes. Furthermore, its antibacterial qualities have led to its use as a preservative [13].

In the realm of tissue regeneration, chitosan-based scaffolds have demonstrated their excellence in promoting the regeneration of hard tissues both in the laboratory and living organisms [14]. Notably, they possess antibacterial properties that disrupt bacterial cell membranes [15]. However, the direct use of pure chitosan for electrospinning presents challenges due to its low solubility, large molecular size, and strong hydrogen bonds [16]. To address these hurdles, researchers have turned to blending chitosan with other natural and synthetic materials, making it more amenable to electrospinning [17].

Poly(ε-caprolactone) (PCL), a stable, non-hazardous, and biodegradable polyester, has found widespread use in various applications [18]. Its excellent mechanical properties and biocompatibility make it suitable for applications ranging from tissue engineering to sutures and drug delivery [19]. However, PCL nanofibers, being inherently hydrophobic, may not be ideal for stimulating cell growth and migration [20]. To tackle this limitation, researchers often opt to blend PCL with chitosan to improve the nanofibers' surface wettability [21].

This study embarks on an innovative path by exploring the application of a water-based cinnamon extract incorporated into polycaprolactone/chitosan nanofibers through electrospinning. The objective is to create a coating for titanium implants that enhances their physical and chemical properties, The ultimate goal is to significantly improve osseointegration, thereby benefiting the field of implantation, wound healing, and tissue engineering. The pharmacological relevance of this research, especially in the context of wound healing and implant coatings, justifies the incorporation of a polymer matrix with plant-based materials.

MATERIALS AND METHODS

Materials

Polycaprolactone (PCL polymer with a molecular weight of Mn = 80,000g/mol) purchased from Sigma Aldrich. Chitosan (CH) with a medium molecular weight (300 - 1000 cps) and a degree of deacetylation of ≥85%, purchased from Glentham Life Science. Acetic acid glacial with a molecular weight of 60.05, provided by Alpha chemika. Formic acid with a molecular weight of 46.03, also provided by Alpha chemika.

Plant extracts preparation

Cinnamon Extract Preparation: Cinnamon bark was finely ground and sifted to obtain a fine powder. 100 g of this powder was mixed with 1 liter of sterile water and heated in a water bath at 60°C for one hour. The mixture was then filtered through sterile filter paper (Whatman, UK) No.1. The filtrate was concentrated under reduced pressure using a rotary vacuum evaporator until it became a semi-solid substance. This substance was further dried at a controlled temperature (45°C) in a convection oven to remove water and obtain a solid powder. The resulting extract had a brown, viscous appearance, with particles averaging about 3.29 micrometers in size, spherical in shape. It was stored at 4°C in a refrigerator until needed [22].

Substrate preparation for vitro study

Experimental Setup for Titanium Discs: For all experiments in this study, commercially pure titanium grade II discs from Smart DEM-Germany were used. These discs had a diameter of 20 mm and a height of 2 mm. To prepare the discs, a polishing machine was utilized along with a sequence of SiC paper with grit sizes of 320, 400, 600, 800, and 1000. Subsequently, the discs underwent two rounds of sonication, each lasting 5 minutes, using acetone, ethanol, and distilled water. After the smoothing process, the discs were left to air dry at room temperature for a duration of 15 minutes [23].

Preparation of electrospinning solutions

Preparation of Polymer Blend with Cinnamon Extract: In accordance with a previous study [24], a polymer blend consisting of 8wt% PCL and 10% chitosan was selected. PCL was dissolved in a mixture of acetic and formic acid (3:7 v/v) using a plate magnetic stirrer for a duration of 3 hours. Subsequently, chitosan was added to the PCL solution and stirred overnight until a clear and homogeneous Chitosan/PCL blend was achieved. The appropriate concentration of the cinnamon watery extract was determined through trials with varying concentrations (10, 15, 20 mg/ml). Afterward, the extract was added to the blend and stirred for 1 hour to create solutions that were further homogenized for 10 minutes using an ultrasonic homogenizer (Model 300VT Ultrasonic Homogenizer, USA). These prepared PCL/Chitosan/cinnamon solutions were then ready for use in the electrospinning coating process.

Electrospinning Fabrication process

Electrospinning Process for PCL/CH/Cinnamon Extract Nanofibers: The prepared PCL/CH solution was loaded into a 5-ml syringe fitted with a blunt-end 0.7 G needle. This solution was dispensed at a controlled rate of 0.6 ml/h using an infusion pump (kd scientific syringe pump 200, USA). The distance between the needle tip and the grounded titanium disc samples was maintained at a constant 15 cm. After experimentation with various voltage settings (15, 20, 25 kV), a high voltage of 25 kV was applied to the needle. The electrospinning process took place in an environment with a relative humidity ranging from 30% to 50%. Once the PCL/CH/Cinnamon extract solution was prepared, it was electrospun under the optimized parameters selected for this study. The resulting samples were air-dried overnight and stored in a desiccator before subsequent analysis.

Table 1 summarizes the key details of the composites and the electrospinning parameters employed in the creation of the samples as outlined in the methods section.

Vitro test

Field Emission-Scanning Electron Microscopy (FE-SEM)

Microstructural Analysis: Following sputtering with gold, the microstructures of Cp Ti and the coatings of PCL/CH and PCL/CH/CN with varying concentrations were examined. This analysis was conducted using a field emission scanning electron microscope (Hitachi SU8020, Japan) operating at an accelerating voltage of 15 kV, utilizing secondary electron (SE) imaging, and maintaining a working distance of 15,800 µm· To characterize

Table 1. The electrospinning settings of fabricated fibrous mats.

Selected Specimen	Conc.	Feed Rate	T.C.D (cm)	Volt
PCL/CH	8%+0.8%	0.6	15	25
PC//CH/CN	8%+0.8%+0.6%	0.6	15	25
PC//CH/CN	8%+0.8%+1.2%	0.6	15	25
PC//CH/CN	8%+0.8%+2.4%	0.6	15	25

the resulting fibers, pore size, and particle size, measurements were taken at random locations on each fiber using Image J software (version 20).

Fourier Transform Infrared spectroscopy (FTIR)

Chemical Bond Analysis: To investigate the chemical bonds present in PCL, CH, CN, and the coating nanofibers, Fourier Transform Infrared Spectroscopy (FTIR) was utilized. The FTIR analysis was conducted using a BRUKER TENSOR-27 IR spectrometer located in the Material Engineering Department laboratory at the University of Technology, Iraq.

For the analysis, the samples were securely attached to the Attenuated Total Reflection (ATR) crystal. The infrared spectra were then recorded across the (4000–650) cm^{-1} spectral range, with a resolution of 4.0 cm^{-1} and 16 scans, using a universal ATR sampling accessory. This allowed for the identification and characterization of the chemical bonds within the studied materials and nanofibers.

Wettability assay

The wettability was tested using deionized distal water and the sessile drop technique (Optical contact angle SL200KS, China). This approach was carried out by dropping 1 ml of distilled water on the coated and control disks and evaluating the contact angle of water for 10 seconds. The

Fig. 1. Position of dental implant (DI) in the rabbit femur.

Fig. 2. Torque removal test.

wettability test was performed in triplicate, and the contact angle was measured using a camera-based contact angle meter.

The atomic force microscope assay (AFM)

AFM is the candidate device to quantify the roughness measurements of a materials` surface of coating and uncoating, it also used to construct 2D and 3D high resolution images of the surfaces which provides additional source of data analysis and quantification. Surface topography and morphology were characterized by atomic force microscopy using TT-2 AFM model. A non-contact mode was used during the AFM examination because the metals have rough surface.

Antibacterial test withe Disc diffusion method (Kirby-Bauer method)

Assessing Antibacterial Activity: The antibacterial properties of the PCL/CH/CN coating were evaluated using the inhibition zone technique. For this study, total anaerobic bacteria isolated from deep pockets of peri-implantitis implants were employed as model microorganisms. To ensure sterility, the disks were exposed to UV light for one hour.

In the experimental setup, Müller-Hinton agar plates were utilized, and they were inoculated with 1 mL of bacterial suspension containing approximately 10^8 colony-forming units (CFU) per milliliter. Both the titanium substrate with the coating and the uncoated controls, each with a 6mm diameter, were gently positioned on the inoculated plates. These plates were then incubated at 37°C for a period of 24 hours.

The zones of inhibition, indicating the antibacterial effect, were quantified by measuring the clear areas surrounding both the coated and uncoated titanium samples [25].

Vivo test

Biomechanical Torque Removal Test

Test Materials: Screws with specific dimensions were utilized for this test, measuring 8mm in length (comprising 5mm threaded and 3mm non-threaded sections) and 3mm in diameter. Each screw featured a central slit, measuring 1mm in width and 1.5mm in depth, to accommodate a screwdriver and torque meter. Two groups were examined: coated dental implants with the PCl/CH/CN composite and uncoated screws. Prior to testing, all components were subjected to sterilization using UV light [26].

Animal Model and Implantation

The biomechanical assessment involved the

Table 2. The electrospinning processing variables for PCL/CH solution.

Flow rate (ml/h)	Voltage (Kv)	Distance (cm)	Fibre production
0.6	15	15	No fibre produced
0.6	20	15	No fibre produced
0.6	25	15	Fibre production

Table 3. The average fiber diameters related to the concentration of cinnamon.

Conc. Cinnamon Mg/ml	Flow rate (ml/h)	Voltage (Kv)	Distance (cm)	Fibre diameter (nm)
10mg/ml	0.6	25	15	Spraying without any fiber
15mg /ml	0.6	25	15	Fibers with bead
20mg//ml	0.6	25	15	Homogenous fiber without any bead

implantation of these screws into the femur bones of 10 male rabbits, each weighing 2 kg. The surgical procedure commenced with the shaving of the external surfaces of the rabbit femurs, followed by a carefully executed lateral incision. Using a 1.3,2.8 mm diameter round bur, two holes were created,

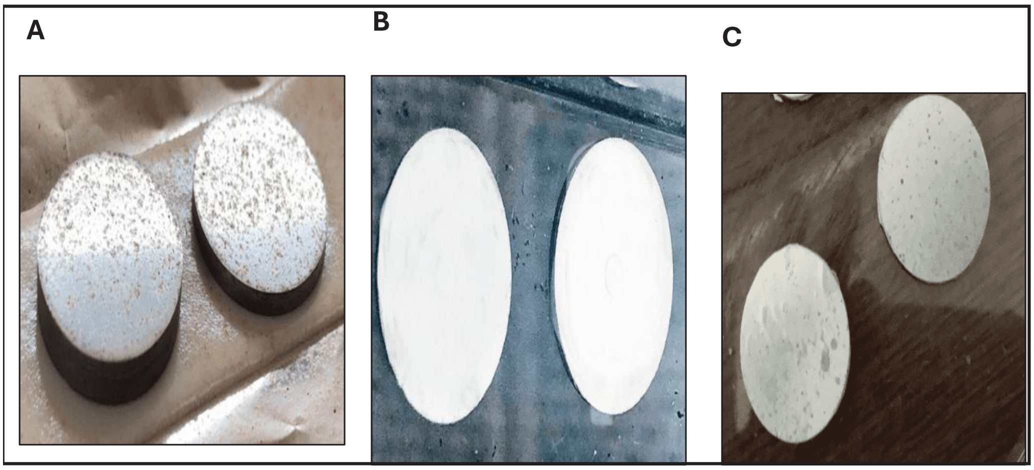

Fig. 3. Optical view of samples electro spinning coating with different concentration CN, A:10mg/ml with spraying, B:15mg/ml white homogenous coating, c: 20mg/ml coating with few drapes of spraying.

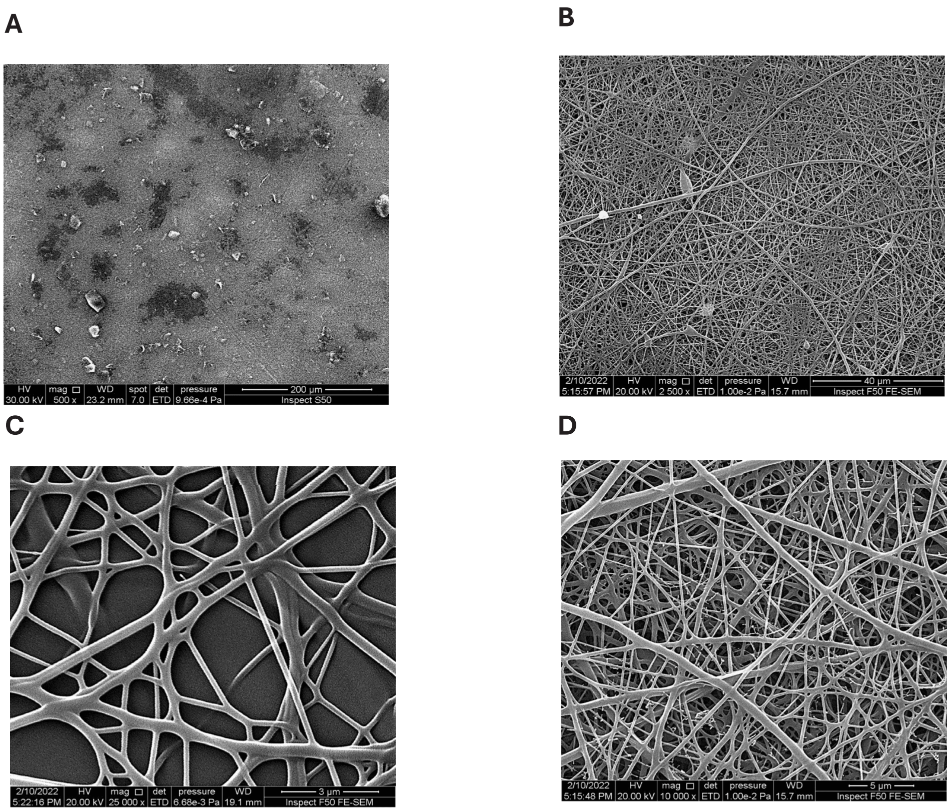

Fig. 4. SEM for PCL/CH with different cinnamon extract concentration A:CN 10mg/ml, B:20mg/ml, C: pcl/CH without CN D:15mg/ml.

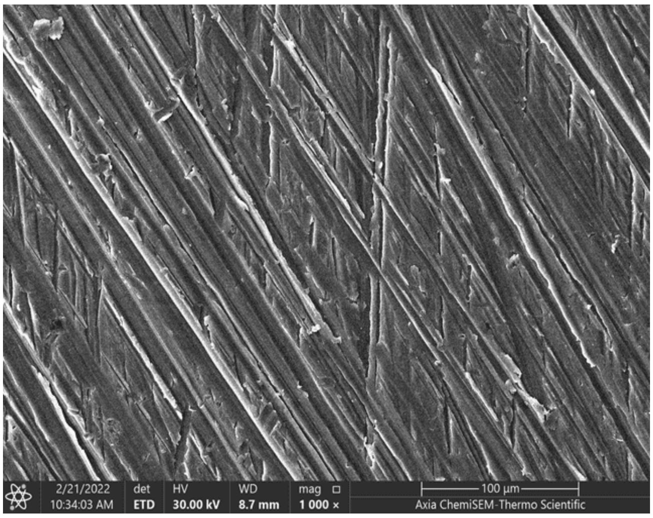

Fig. 5. SEM for uncoated titanium substrate at different magnification. A: magn. 4000 , B: magn. 2000, C: magn. 1000×.

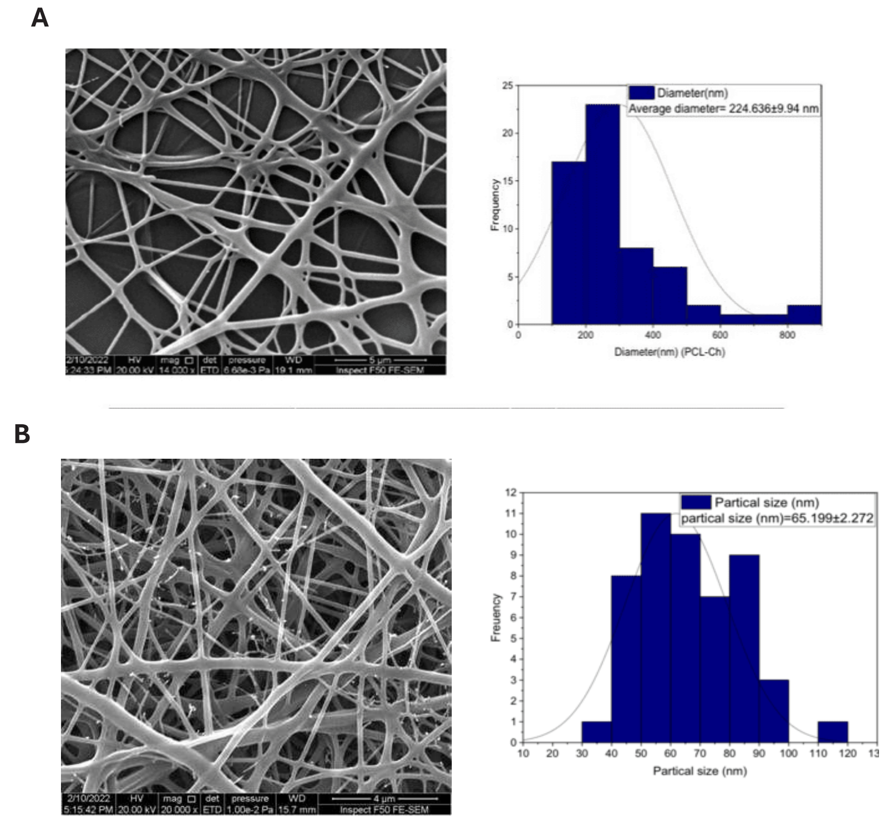

`Fig. 6. SEM morphology with histogram of fibers diameter and distributions for A: PCL/ CH nanofibers B: PCL/CH/CN fiber.

positioned 1 cm apart. In these holes, the coated screws were inserted into the upper hole, while the uncoated screws were placed in the lower hole for each femur of rabbit. they were implanted in rabbit femurs for 2 and 6 weeks for biomechanical assessment. 10 screws/group were tested by this test [27] as shown with Fig. 1.

Biomechanical Testing

Subsequently, the removal torque test was conducted on these implanted screws. using a removal torque tester (professional torque meter, TQ 8800, Mrclab, China) [26] as shown with Fig. 2.

Statistical analysis

The data obtained from the characterization were analyzed using IBM SPSS software (ver. 23, SPSS Inc., IL, USA). By using T test for Significant Difference (difference between the means of the two groups). The level of significance was set at p-values less than 0.05. All experimental data are presented as mean ± standard deviation (SD).

RESULTS AND DISCUSSION

Optimization of electrospinning parameters and cinnamon extraction

The Table 2 shows the results for different

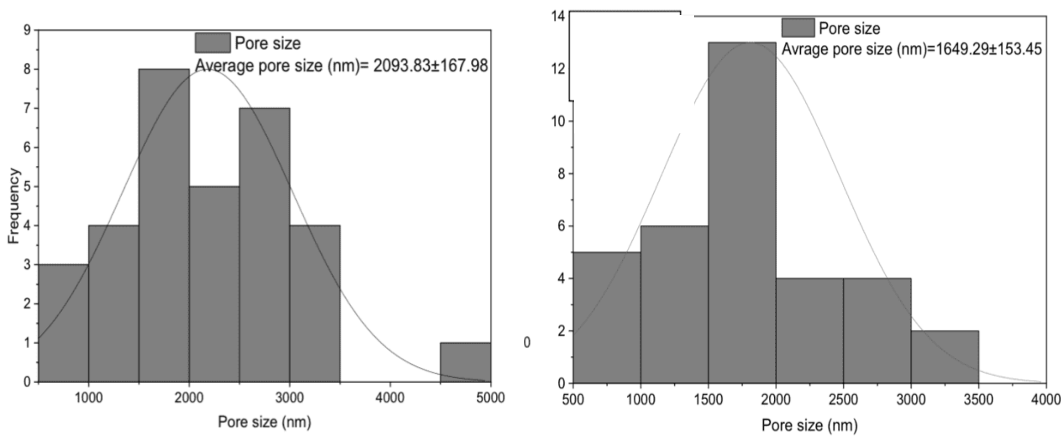

A **B**

Fig. 7. Histogram for average pore size for A: PCL/CH B: PCL/CH/CN.

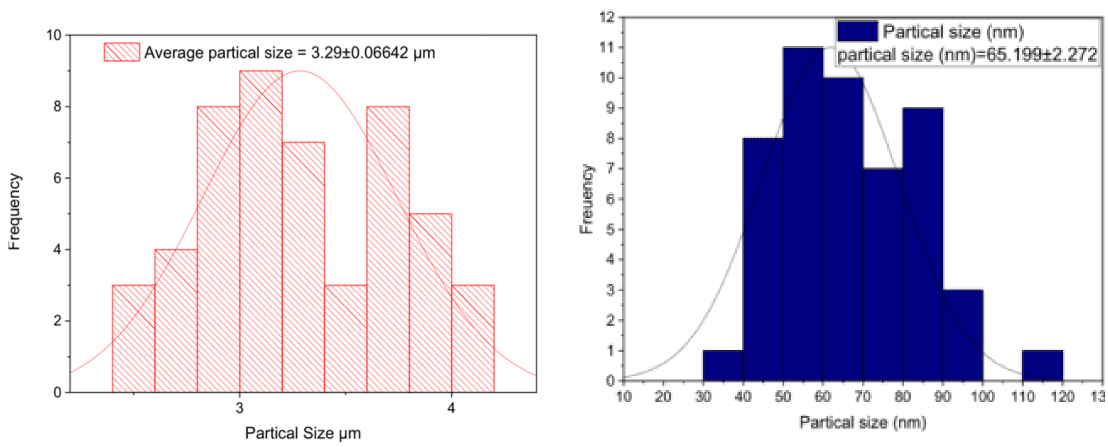

A **B**

Fig. 8. Histogram for cinnamon particle size and distribution A: before electrospinning. B: after electrospinning.

combinations of flow rate, voltage, and distance. At a flow rate of 0.6 ml/h and a voltage of 25 KV with a fixed distance of 15 cm, fiber production was achieved. This combination of parameters was selected for further experiments involving different concentrations of cinnamon. Table 3 and Fig. 3 provide additional details on the chosen concentration of cinnamon extract and visual representation of the fibers produced. However, when incorporating different concentrations of CN into PCL/CH, distinct results were obtained. For a CN concentration of 10 mg/ml, no fiber formation occurred. At 20 mg/ml CN concentration, spindle-shaped beaded fibers were observed. It was only at a CN concentration of 15 mg/ml that bead-free, homogeneously distributed non-woven fibers were achieved as shown with Fig. 4.

Field-emission scanning electron microscopy (FESEM)

Observations of Fiber Characteristics: The surface of the titanium substrate, as depicted in Fig. 5, exhibited numerous valleys and grooves. These surface features were a direct outcome of the grinding process involving SiC paper.

In the case of PCL/CH fibers, uniform and bead-free non-woven fibers were observed. These fibers exhibited a diameter ranging from 100 to 900 nm, with a mean diameter of 224 ± 9.94 nm as are shown with Fig. 6A. The average pore size was measured to be 2.093.83 ± 167.98 nm, as depicted in Fig. 7A. The PCL/CH/CNT fibers exhibited a diameter ranging from 50 to 550 nm, with a mean diameter of 178.66 ± 17.55 nm as shown with Fig. 6B, the average porosity was measured to be 1649.29 ± 153.45 nm, as illustrated in the histogram in Fig. 7B.

Furthermore, the cinnamon particles were evenly distributed with an average particle size of 65.199 ± 2.272 nm, as demonstrated in Fig. 8.

Fourier Transform Infrared spectroscopy (FTIR)

FTIR Analysis of PCL, Chitosan, Cinnamon, and Coating in Electrospun Fibers: In Fig. 9, we present the FTIR spectra of various components, including PCL, CS (Chitosan), cinnamon, and the PCL/CS/cinnamon coating within electrospun fibers. These spectra provide valuable information about the

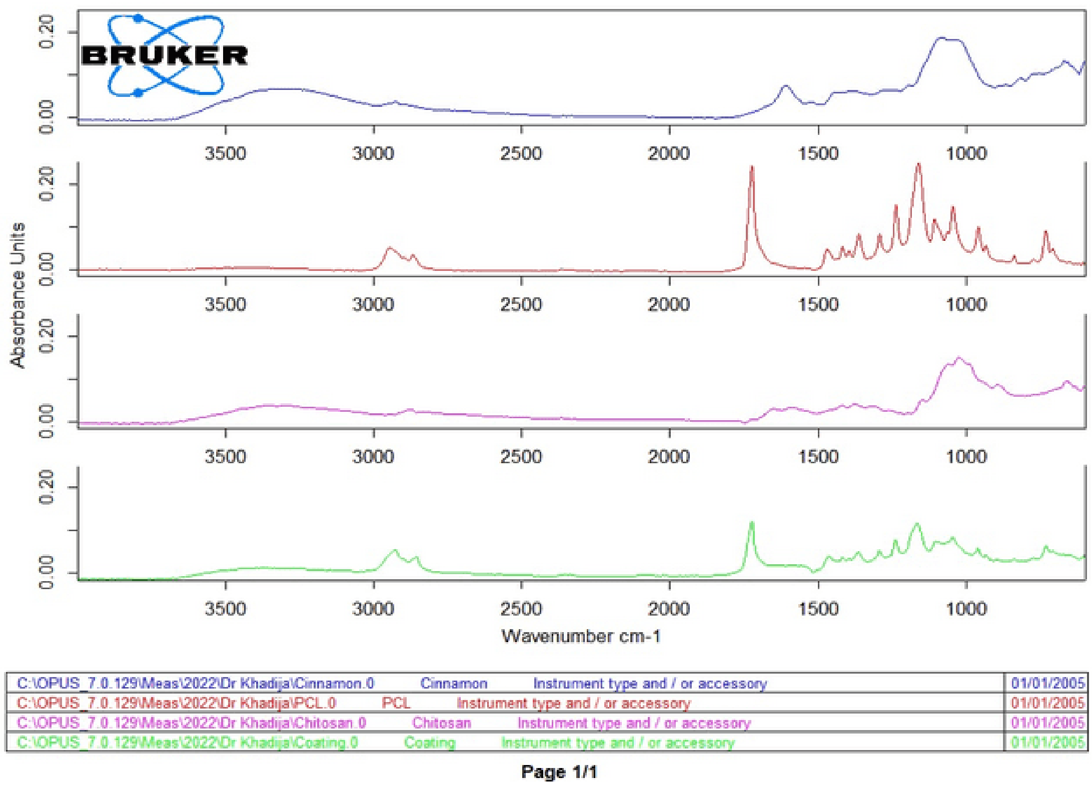

Fig. 9. FTIR spectra of polycaprolactone (PCL), chitosan (CH). Cinnamon extract (Cn), and PCL/CH/Cn composite nanofibers.

chemical composition of the materials.

PCL Spectrum: The spectrum of pristine PCL exhibits a prominent peak at 1723 cm^{-1}, corresponding to the carbonyl group of the ester. Additionally, it displays an asymmetric CH2 stretching peak at 2943 cm^{-1} and a symmetric CH_2 stretching peak at 2869 cm^{-1}. The absorption peak at 1292 cm^{-1} is attributed to C–O and C–C stretching modes, with bands at 1237 and 1161 cm^{-1} related to asymmetric and symmetric C–O–C stretching [28].

CS Spectrum: The FTIR spectrum of chitosan demonstrates peaks at 3293 cm^{-1}, representing OH and NH stretching, and a band between 1636–1650 cm^{-1} corresponding to C=O stretching (amide-I). Another peak at 1587 cm^{-1} is attributed bending vibration, C-O-C stretching to the C=O stretching (amide-I). Peaks at 1418, 1150, and 1025 cm^{-1} represent CH_3 vibration, and C-OH bending vibration, respectively [29,30].

Cinnamon Spectrum: The spectrum of pure cinnamon displays a broad peak at 3404 cm^{-1}, indicating the presence of free hydroxyl groups and hydroxyl groups involved in hydrogen bonding. Peaks between 3400 and 3600 cm^{-1} are associated with the vibrational O-H of hydroxyl groups, and a band at 2930-2925 cm^{-1} is attributed to the asymmetric stretching vibration of C-H in methylene and methyl groups. There's a peak at 1440-1450 cm^{-1} characterizing the C–OH group's bending vibration, while a transmittance peak at 1500-1525 cm^{-1} represents the C=O aromatic structure. Additionally, a band at 1434 cm^{-1} arises from the C=C stretching vibration in aromatic rings, which can be found in phenolic and flavonoid compounds [31].

Coating Spectrum: In the FTIR spectrum of the coating, a broad, low-intensity peak at 3404 cm^{-1} indicates NH and OH vibrations from chitosan or CN, while a high-intensity peak at 1732 cm^{-1} is associated with PCL. There are also low-intensity peaks at 1500-1525 cm^{-1}, possibly originating from aromatic rings, which may belong to cinnamon.

Water Contact Angle Analysis

In Fig. 10, water contact angle measurements

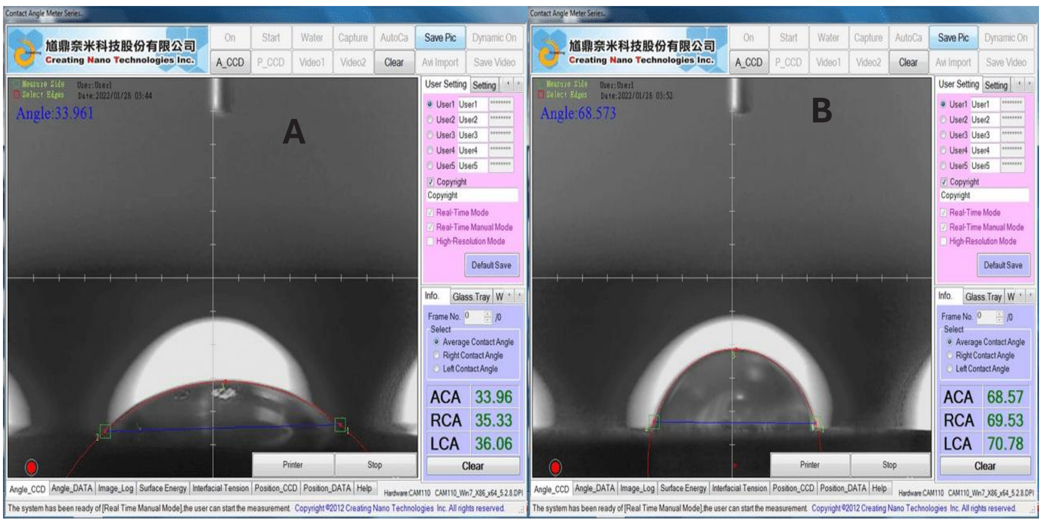

Fig. 10. Water contact angle measure A: -coating sample, B: control samp

Table 4. Descriptive analysis for control and coating sample andT-test comparison between coating and control sample by student test at value<0.05.

Group	N.	Mean	Std.Deviation	Std.Error	T	df	Sig. (2-tailed)
Control	10	66.4	3.170	1.1	9.246	18	.000
Coated	10	42.9	7.36	2.3	9.246	12.3	.000

were presented for both the control and coating groups. The control group exhibited contact angles ranging from 62.18°C to 73.41°C, with a mean of 66.39°C ± 3.17°C. In contrast, the coating group had contact angles ranging from 30.03°C to 43.0°C, with a mean of 42.96°C ± 7.3°C.

A statistical analysis using the T-test (shown in Table 4) demonstrated a highly significant difference between the coated surfaces and the uncoated group.

Atomic Force Microscopy (AFM) Surface Analysis:

For the examination of surface morphology and surface roughness, AFM was mployed to analyze two groups: uncoated titanium samples and nano-fiber coated titanium samples. The 3D and 2D images of both groups are visually depicted in Fig. 11.A comparison of the mean values of surface roughness(Sa) for these two groups is summarized in Table 5, which highlights that the coating group exhibited the highest mean surface

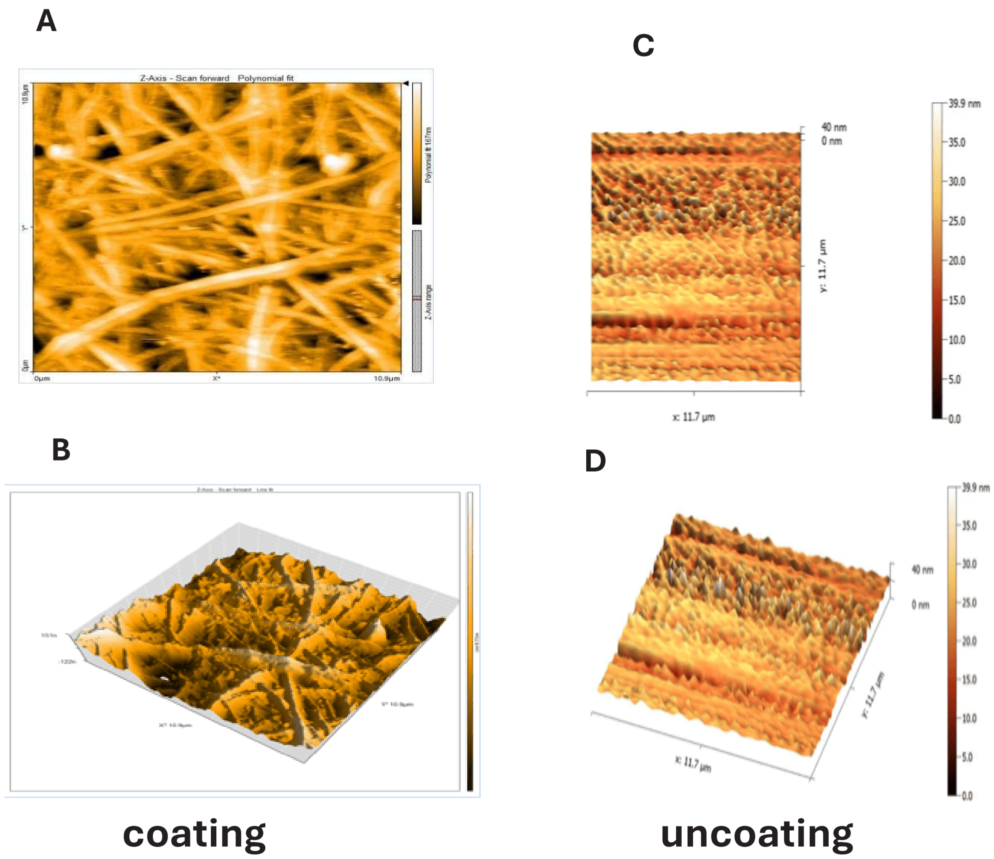

Fig. 11. Atomic force microscopy (AFM) 2D,3D topographical images of control and coated samples.

Table 5. Statistical analysis for surface roughness between control and coating sample. descriptive analysis. And t test for comparison between two groups at P value less than0.05.

Group Statistics					Independent Samples Test		
Group	N	Mean	Std. Deviation	Std. Error Mean	t	df	Sig. (2-tailed)
Control	5	0.15280	0.007014	0.003137	-29.266	8	00
Coating	5	1.155	0.068191	0.03496	-29.266	4.1	.000

roughness values.

The antibacterial Activity Assessment:

The PCL/CH/CN composite demonstrated a significant antibacterial effect by inducing the formation of an inhibition zone measuring 36.9 ± 5.5 mm against bacterial growth. In contrast, the control groups exhibited no inhibition zones, as illustrated in Table 6 and Fig. 12. This result underscores the potent antibacterial properties of the PCL/CH/CN composite.

Result of vivo test

In the study, all animals showed excellent postoperative healing with no notable side effects. Throughout the study period, they exhibited normal movement without any signs of inflammation, infection, or allergic reactions at the surgical site. The intervention procedures had no impact on the animals' overall health, behavior, or feeding habits. Additionally, the screws used in the procedure remained securely in place and could not be moved manually.

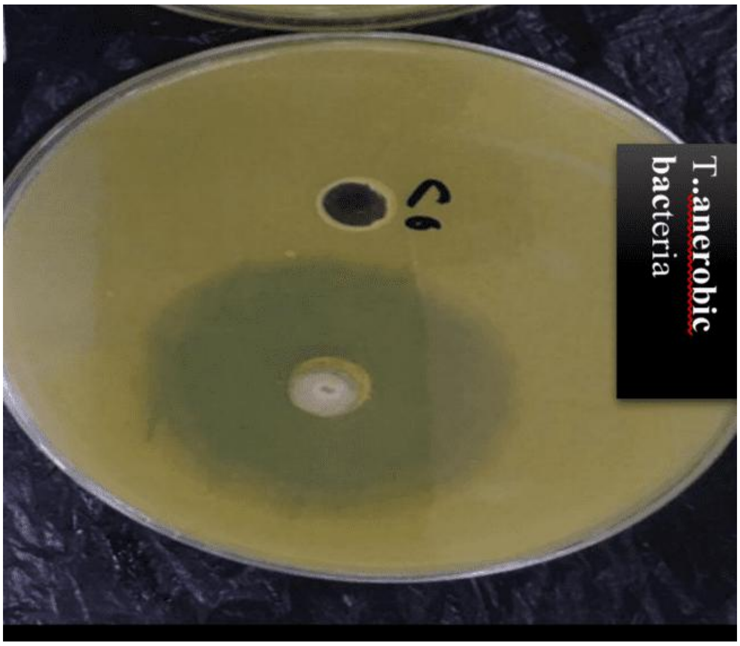

Fig. 12. Zone of inhibition (mm) of coating and control samples against test bacteria on Mueller-Hinton agar medium.

Table 6. Zone of inhibition (mm) of coating and control samples against test bacteria on Mueller-Hinton agar medium.

Group	Bacterial inhibition zone (mm) mean
Coating	36.9
Control	0

Table 7: Descriptive statistics of Torque 2w between groups.

Groups	Mean	±SD	±SE	Minimum	Maximum	t	p.value	Sig. (2-tailed)
Coating	12.2840	0.67822	.21447	11.32	13.45			
Control	10.0060	0.69500	.21978	8.90	11.00	7.418	0.000	H.S
Total	11.1450	1.34621	.30102	8.90	13.45			

Torque removal test

The Torque values of both coated and uncoated samples after 2 weeks are displayed in Table 8. Interestingly, the mean value for the coated samples increased to (12.2840 ± 0.67822), whereas the uncoated samples exhibited lower mean values (10.0060 ± 0.69500). This difference was statistically significant with a p-value of 0.0001.

The removal torque values of both coated and uncoated samples after 6 weeks are presented in Table 8. This observed difference was highly significant with a p-value of 0.0001.

The study utilized electrospinning; a versatile technique known for its ability to create nanofibrous structures. The choice of PCL, CH, and CN in the composite coating was well-considered. PCL contributes to surface roughness while CH and CN provide hydrophilicity and antibacterial properties. This strategic combination addresses multiple aspects critical to enhancing implant osseointegration.

Introduction to Electrospinning Parameters: The choice of voltage during electrospinning is a crucial factor influencing fiber quality. Higher voltage can reduce bead defects and create more uniform fibers [32], this observation aligns with the findings of previous research, which have indicated that the number of beaded fibers tends to decrease as the applied voltage is increased [30]. Essentially, a higher voltage imparts more electrical force to the polymer solution, aiding in the stretching and thinning of the solution during the electrospinning process. This leads to a reduction in bead formation and the production of more uniform fibers [33].

Incorporating Cinnamon Extract: In our study, we aimed to incorporate cinnamon extract into the electrospinning process at different concentrations (10, 15, and 20 mg/ml). However, using the lowest concentration (10 mg/ml) with the PCL/CH polymer resulted in electrospraying due to low viscosity. Electrospraying produces droplets instead of continuous fibers, which is undesirable [34]. To overcome electrospraying, we selected a slightly higher concentration (15 mg/ml) for cinnamon extract. This concentration provided the right viscosity and surface tension for successful electrospinning, yielding uniform and continuous fibers [35].

Pore Size and Porosity Considerations: Porosity plays a crucial role in nanofibers' functions, influencing fluid transport, water absorption, chemical release, and biochemical interactions [36]. Our study observed that PCL/CH/CN coatings had smaller pores compared to PCL/CH coating, likely due to cinnamon particles interacting within these pores [36].

Herbal extracts like cinnamon contain various components such as tannins, phenols, and minerals like magnesium, chloride, sulfate, and nitrate [37]. These components can influence the electrical conductivity of materials [38] that may be contributed to formation the smallest fiber diameter which are are considered significant in terms of their fiber morphologies. Other studies have concluded that non-woven nanofibrous membrane mats used for wound healing should have pore sizes ranging from 500 nm to 1 mm. These pore sizes are small enough to prevent bacterial penetration through aerosol particle capturing mechanisms. Additionally, these nanofibers provide a high surface area, which is highly efficient for fluid absorption. and delivery [39]. The microarchitecture of these fibers' mimics that of the extracellular matrix, which can enhance cell adhesion, proliferation, migration, and differentiation [40].

Surface Roughness Enhancement: The electrospinning process introduced changes in surface roughness. Rougher implant surfaces promote better attachment and stability by enhancing bone interlocking. Our study found that the coating's roughness fell within the optimal range for promoting mineralized bone-implant interaction [41,42]. This increase in roughness could be attributed to the electrospinning process, which creates valleys and peaks within the membrane fiber coating.

The electrospinning process transformed

Table 8. Descriptive statistics of Torque 6 w between groups.

Groups	Mean	±SD	±SE	Minimum	Maximum	t	p.value	Sig. (2-tailed)
Coating	30.4220	1.15897	.36650	28.98	33.12	15.262	0.000	H.S
Control	22.2010	1.24835	.39476	19.90	24.00			
Total	26.3115	4.37721	.97877	19.90	33.12			

cinnamon particles from a micro to a nano size and this may be contributed to increase Sa of coating. The presence of nano-sized cinnamon particles in the coating might positively influence cell growth and osteoblastic differentiation on the implant surface. This could contribute to improved bone integration and overall implant success. Moreover, nano-sized cinnamon particles may possess antibacterial properties, potentially inhibiting the colonization of bacteria on the implant surface. This antibacterial effect aligns with the goal of reducing the risk of infection and promoting faster healing before implant loading.and this agree with thus facilitating quicker healing prior to loading as elucidated by Deng et al. in 2015 [43]. This observation aligns with the findings of GH Jani and AA Fatalla in 2022 and Eom et al. in 2012 [44,45], whom noted a significant increase in surface roughness when coated with materials featuring nano or micro-sized particle.

Synergistic Antibacterial Effects of combination of chitosan and cinnamon in our coating enhanced its antibacterial effects. Cinnamon's cinnamaldehyde compound interferes with bacterial growth, complementing chitosan's antimicrobial properties [46].

Incorporating hydrophilic components like chitosan and cinnamon extract into the electrospun composite improved the traditionally hydrophobic titanium surface's hydrophilicity. This enhancement is beneficial for biological compatibility and implant performance in a physiological environment.

both the present study and the study by Agnes Mary et al. demonstrate a trend where the incorporation of natural plant extracts, such as Aloe vera, into PCL nanofibrous scaffolds leads to improved hydrophilicity [47,48].

In the FTIR spectrum of the coating, comprising PCL, chitosan, and possibly cinnamon, the absence of new, significant peaks or shifts suggests that there are no strong chemical reactions occurring among these components [49]. Instead, the spectrum reveals that the coating primarily involves physical interactions between the individual constituents.

The increase in torque following coating can be attributed to heightened hydrophilicity, surface roughness enhancement, and antibacterial properties. After six weeks, bone maturation likely contributed to improved implant stability and compatibility with biological system [50,51].

Overall, these results underscore the coating's positive influence, enhancing implant compatibility with biological systems and facilitating seamless integration with surrounding bone. Enhanced surface characteristics, marked by increased roughness and enhanced wettability, expedite and reinforce bone tissue attachment, thereby promoting superior osteoconduction [52,53].

CONCLUSION

The study found that the PCL/CH/CN coating significantly improved the surface properties of titanium, including surface morphology, chemical bioactive structure, roughness, and wettability. The electrospinning coating method used in the study produced nanoparticles that increased surface roughness and wettability. The coating also created a high surface contact area and porosity, which improved the interaction with physiological medium and promoted cell adhesion, proliferation, and differentiation. The water contact angle measurements showed that the coated surface was more hydrophilic than the uncoated surface. Additionally, the study confirmed the antibacterial activity of the PCL/CH/CN fiber coating against anaerobic bacteria associated with perimplantitis. These findings suggest that the PCL/CH/CN coating has the potential to enhance osseointegration and may be beneficial for implant success.

CONFLICT OF INTEREST

The authors declare that there is no conflict of interests regarding the publication of this manuscript.

REFERENCES

1. Bachtiar E, Jujur I, Damisih, Devy K, Suha S, Bachtiar B. Effect of implantation Ti-6Al-4V ELI in femoral bone defect regeneration of Sprague Dawley rat. Journal of Advanced Pharmaceutical Technology and Research. 2020;11(4):202.
2. Nhlapo N, Dzogbewu TC, de Smidt O. Nanofiber Polymers for Coating Titanium-Based Biomedical Implants. Fibers. 2022;10(4):36.
3. Bohara S, Suthakorn J. Surface coating of orthopedic implant to enhance the osseointegration and reduction of bacterial colonization: a review. Biomaterials Research. 2022;26(1).
4. Liu H, Bai Y, Huang C, Wang Y, Ji Y, Du Y, et al. Recent Progress of Electrospun Herbal Medicine Nanofibers. Biomolecules. 2023;13(1):184.
5. Chopra D, Gulati K, Ivanovski S. Understanding and optimizing the antibacterial functions of anodized nano-engineered titanium implants. Acta Biomater. 2021;127:80-101.
6. Tian F, Hosseinkhani H, Hosseinkhani M, Khademhosseini A, Yokoyama Y, Estrada GG, et al. Quantitative analysis of cell adhesion on aligned micro- and nanofibers. Journal of

Biomedical Materials Research Part A. 2007;84A(2):291-299.
7. Huesca-Urióstegui K, García-Valderrama EJ, Gutierrez-Uribe JA, Antunes-Ricardo M, Guajardo-Flores D. Nanofiber Systems as Herbal Bioactive Compounds Carriers: Current Applications in Healthcare. Pharmaceutics. 2022;14(1):191.
8. Trifan A, Zengin G, Brebu M, Skalicka-Woźniak K, Luca SV. Phytochemical Characterization and Evaluation of the Antioxidant and Anti-Enzymatic Activity of Five Common Spices: Focus on Their Essential Oils and Spent Material Extractives. Plants. 2021;10(12):2692.
9. Mohammadi M, Mirabzadeh S, Shahvalizadeh R, Hamishehkar H. Development of novel active packaging films based on whey protein isolate incorporated with chitosan nanofiber and nano-formulated cinnamon oil. Int J Biol Macromol. 2020;149:11-20.
10. Hariri M, Ghiasvand R. Cinnamon and Chronic Diseases. Advances in Experimental Medicine and Biology: Springer International Publishing; 2016. p. 1-24.
11. Sebai H, Rtibi K, Selmi S, Jridi M, Balti R, Marzouki L. Modulating and opposite actions of two aqueous extracts prepared from Cinnamomum cassia L. bark and Quercus ilex L. on the gastrointestinal tract in rats. RSC Advances. 2019;9(38):21695-21706.
12. Tran N, Pham B, Le L. Bioactive Compounds in Anti-Diabetic Plants: From Herbal Medicine to Modern Drug Discovery. Biology. 2020;9(9):252.
13. Yahya EB, Abdul Khalil HPS, Ahmad MI, Rizal S, Muhammad S. Cleaner approach of preparing antibacterial bioaerogel scaffolds using oil palm waste nanocellulose. Industrial Crops and Products. 2023;191:115897.
14. Islam MM, Shahruzzaman M, Biswas S, Nurus Sakib M, Rashid TU. Chitosan based bioactive materials in tissue engineering applications-A review. Bioactive Materials. 2020;5(1):164-183.
15. Qasim S, Zafar M, Najeeb S, Khurshid Z, Shah A, Husain S, et al. Electrospinning of Chitosan-Based Solutions for Tissue Engineering and Regenerative Medicine. Int J Mol Sci. 2018;19(2):407.
16. Yin J, Xu L. Batch preparation of electrospun polycaprolactone/chitosan/aloe vera blended nanofiber membranes for novel wound dressing. Int J Biol Macromol. 2020;160:352-363.
17. Zhang Z, Liu H, Yu D-G, Bligh S-WA. Alginate-Based Electrospun Nanofibers and the Enabled Drug Controlled Release Profiles: A Review. Biomolecules. 2024;14(7):789.
18. Dwivedi R, Kumar S, Pandey R, Mahajan A, Nandana D, Katti DS, et al. Polycaprolactone as biomaterial for bone scaffolds: Review of literature. Journal of Oral Biology and Craniofacial Research. 2020;10(1):381-388.
19. Al-Musawi S, Albukhaty S, Al-Karagoly H, Almalki F. Design and Synthesis of Multi-Functional Superparamagnetic Core-Gold Shell Nanoparticles Coated with Chitosan and Folate for Targeted Antitumor Therapy. Nanomaterials. 2020;11(1):32.
20. Kahdim QS, Abdelmoula N, Al-Karagoly H, Albukhaty S, Al-Saaidi J. Fabrication of a Polycaprolactone/Chitosan Nanofibrous Scaffold Loaded with Nigella sativa Extract for Biomedical Applications. BioTech. 2023;12(1):19.
21. American Dental Association/Federation Dentaire Internationale Joint 1988 World Dental Congress preliminary program. The Journal of the American Dental Association. 1988;117(1):21-145.
22. Al-dhaher ZA. THE ANTIBACTERIAL ACTIVITY OF AQUEOUS EXTRACT OF CINNAMON AND CLOVE AGAINST STAPHYLOCOCCUS AUREUS. Journal of Al-Nahrain University Science. 2008;11(2):131-135.
23. Jani GH, Al-Ameer SS, Jawad BDS. Histological and Histomorphometric Analysis of Strontium Chloride Coated Commercially Pure Titanium Implant Compared with Hydroxyapatite Coating. Journal of Baghdad College of Dentistry. 2015;27(1):26-31.
24. Jorgensen JH, Pfaller MA. Introduction to the 11th Edition of the Manual of Clinical Microbiology. Manual of Clinical Microbiology: ASM Press; 2015. p. 1-4.
25. Mahmood MS, Al-Ameer SS. Assessment of Calcium Carbonate Coating on Osseointegration of Commercially Pure Titanium Implant by Torque Removal Test and Histomorphometric Analysis. Journal of Baghdad College of Dentistry. 2017;29(1):32-38.
26. Abdullah ZS, Mahmood MS, Abdul-Ameer FMA, Fatalla AA. Effect of commercially pure titanium implant coated with calcium carbonate and nanohydroxyapatite mixture on osseointegration. J Med Life. 2023;16(1):52-61.
27. Van der Schueren L, Steyaert I, De Schoenmaker B, De Clerck K. Polycaprolactone/chitosan blend nanofibres electrospun from an acetic acid/formic acid solvent system. Carbohydr Polym. 2012;88(4):1221-1226.
28. Tayebi T, Baradaran-Rafii A, Hajifathali A, Rahimpour A, Zali H, Shaabani A, et al. Biofabrication of chitosan/chitosan nanoparticles/polycaprolactone transparent membrane for corneal endothelial tissue engineering. Sci Rep. 2021;11(1).
29. Alyamani AA, Al-Musawi MH, Albukhaty S, Sulaiman GM, Ibrahim KM, Ahmed EM, et al. Electrospun Polycaprolactone/Chitosan Nanofibers Containing Cordia myxa Fruit Extract as Potential Biocompatible Antibacterial Wound Dressings. Molecules. 2023;28(6):2501.
30. Ahmed Ismail K, El Askary A, Farea MO, Awwad NS, Ibrahium HA, Eid Moustapha M, et al. Perspectives on composite films of chitosan-based natural products (Ginger, Curcumin, and Cinnamon) as biomaterials for wound dressing. Arabian Journal of Chemistry. 2022;15(4):103716.
31. Roozbahani F, Sultana N, Fauzi Ismail A, Nouparvar H. Effects of Chitosan Alkali Pretreatment on the Preparation of Electrospun PCL/Chitosan Blend Nanofibrous Scaffolds for Tissue Engineering Application. Journal of Nanomaterials. 2013;2013(1).
32. Liu Y, Dong L, Fan J, Wang R, Yu JY. Effect of applied voltage on diameter and morphology of ultrafine fibers in bubble electrospinning. J Appl Polym Sci. 2010;120(1):592-598.
33. Nauman S, Lubineau G, Alharbi HF. Post Processing Strategies for the Enhancement of Mechanical Properties of ENMs (Electrospun Nanofibrous Membranes): A Review. Membranes. 2021;11(1):39.
34. Croitoru A-M, Ficai D, Ficai A, Mihailescu N, Andronescu E, Turculet S. Nanostructured Fibers Containing Natural or Synthetic Bioactive Compounds in Wound Dressing Applications. Materials. 2020;13(10):2407.
35. Nezarati RM, Eifert MB, Cosgriff-Hernandez E. Effects of Humidity and Solution Viscosity on Electrospun Fiber Morphology. Tissue Engineering Part C: Methods. 2013;19(10):810-819.
36. Cao X, Chen W, Zhao P, Yang Y, Yu D-G. Electrospun Porous Nanofibers: Pore−Forming Mechanisms and Applications for Photocatalytic Degradation of Organic Pollutants in Wastewater. Polymers. 2022;14(19):3990.

37. Saad R, Khan J, Krishnanmurthi V, Asmani F, Yusuf E. Effect of Different Extraction Techniques of Persicaria odorata Extracts Utilizing Anti-bacterial Bioassay. British Journal of Pharmaceutical Research. 2014;4(18):2146-2154.
38. Ali HS, Saad R, Elhaj BMA, Khan J, Kaleemullah M, Al-Dhalli S. Effect of Different Parameters on the Release of Diclofenac Modified Tablets. International Journal of Current Pharmaceutical Review and Research. 2017;8(02).
39. Angammana CJ, Jayaram SH. Analysis of the Effects of Solution Conductivity on Electrospinning Process and Fiber Morphology. IEEE Transactions on Industry Applications. 2011;47(3):1109-1117.
40. de Cassan D, Becker A, Glasmacher B, Roger Y, Hoffmann A, Gengenbach TR, et al. Blending chitosan-g-poly(caprolactone) with poly(caprolactone) by electrospinning to produce functional fiber mats for tissue engineering applications. J Appl Polym Sci. 2019;137(18).
41. Kriegel C, Arrechi A, Kit K, McClements DJ, Weiss J. Fabrication, Functionalization, and Application of Electrospun Biopolymer Nanofibers. Critical Reviews in Food Science and Nutrition. 2008;48(8):775-797.
42. Kligman S, Ren Z, Chung C-H, Perillo MA, Chang Y-C, Koo H, et al. The Impact of Dental Implant Surface Modifications on Osseointegration and Biofilm Formation. Journal of Clinical Medicine. 2021;10(8):1641.
43. Wei S, Deng Y, Liu X, Xu A, Wang L, Luo Z, et al. Effect of surface roughness on osteogenesis in vitro and osseointegration in vivo of carbon fiber-reinforced polyetheretherketone/nanohydroxyapatite composite. International Journal of Nanomedicine. 2015:1425.
44. Jani GH, Fatalla AA. Surface Characterization of PEKK Modified by stron-tium–hydroxyapatite coating as implant material Via the magnetron sputtering Deposition technique. Journal of Baghdad College of Dentistry. 2022;34(2):25-36.
45. Eom T-G, Jeon G-R, Jeong C-M, Kim Y-K, Kim S-G, Cho I-H, et al. Experimental study of bone response to hydroxyapatite coating implants: bone-implant contact and removal torque test. Oral Surgery, Oral Medicine, Oral Pathology and Oral Radiology. 2012;114(4):411-418.
46. Pajoumshariati S, Yavari SK, Shokrgozar MA. Physical and Biological Modification of Polycaprolactone Electrospun Nanofiber by Panax Ginseng Extract for Bone Tissue Engineering Application. Ann Biomed Eng. 2015;44(5):1808-1820.
47. Agnes Mary S, Giri Dev VR. Electrospun herbal nanofibrous wound dressings for skin tissue engineering. The Journal of The Textile Institute. 2014;106(8):886-895.
48. Kearns VR, McMurray RJ, Dalby MJ. Biomaterial surface topography to control cellular response: technologies, cell behaviour and biomedical applications. Surface Modification of Biomaterials: Elsevier; 2011. p. 169-201.
49. Callister W, Rethwisch D. A New Paradigm for Learning the Fundamentals of Materials Science and Engineering. 2023 ASEE Annual Conference and Exposition Proceedings: ASEE Conferences.
50. Wang Q, Zhou P, Liu S, Attarilar S, Ma RL-W, Zhong Y, et al. Multi-Scale Surface Treatments of Titanium Implants for Rapid Osseointegration: A Review. Nanomaterials. 2020;10(6):1244.
51. Escobar M. Polymer coatings based on sulfonated-poly-ether-ether-ketone films for Implant Dentistry Applications. Morressier; 2018.
52. Azzawi ZGM, Hamad TI, Kadhim SA, Naji GA-H. Osseointegration evaluation of laser-deposited titanium dioxide nanoparticles on commercially pure titanium dental implants. J Mater Sci Mater Med. 2018;29(7).
53. Kadhim DR, Hamad TI, Fatalla AA. Use of Eggshells as Bone Grafts around Commercially Pure Titanium Implant Screws Coated with Nano Calcium Sulfate. International Journal of Biomaterials. 2022;2022:1-8.